

Communication

# Effects of Solids Accumulation on Greenhouse Gas Emissions, Substrate, Plant Growth and Performance of a Mediterranean Horizontal Flow Treatment Wetland

Alessandro Sacco <sup>1</sup>, Liviana Sciuto <sup>2</sup>, Feliciana Licciardello <sup>1,\*</sup>, Giuseppe L. Cirelli <sup>1</sup>, Mirco Milani <sup>1</sup>  
and Antonio C. Barbera <sup>1</sup>

<sup>1</sup> Dipartimento Agricoltura, Alimentazione e Ambiente (Di3A)—University of Catania, 95124 Catania, Italy

<sup>2</sup> International Doctorate in Agricultural, Food and Environmental Science—Di3A—University of Catania, Via S. Sofia 100, 95123 Catania, Italy

\* Correspondence: feliciana.licciardello@unict.it; Tel.: +39-095-7147551

**Abstract:** In treatment wetlands (TWs), solids accumulation can result in hydraulic malfunction, reducing the operation life, and it could enhance biological activity by favoring biofilm development. It is still unknown whether the solids accumulation can affect greenhouse gas (GHG) emissions. This study aims to evaluate the solid concentration along a horizontal flow (HF) TW, and its role in GHG emissions, hydraulics, treatment performance, and vegetation development (*Phragmites australis* (Cav.) Trin. ex Steud.). The study was carried out in an eight-year-old full-scale HF-TW located in the Mediterranean region (Sicily, Italy). To collect data inside the HF unit, nine observation points (besides the inlet and the outlet) along three 8.5-m-long transects (T1, T2, and T3) were identified. The first transect (close to the inlet zone) showed a hydraulic conductivity ( $K_s$ ) reduction approximately one order of magnitude higher than the other two. Results highlighted that GHG emissions increased during the summer, when the temperature and solar radiation were higher than in the rest of the year, matching the macrophyte growth rate. Theoretical methane ( $\text{CH}_4$ ) emissions followed the trend of volatile solids (VS), which was around 3.5 and 4 times in T1 to T2 and T3. Pore clogging affected carbon dioxide ( $\text{CO}_2$ ) emissions, which decreased from T1 to T3, with maximum monthly values in T1 ( $21.4 \text{ g CO}_2 \cdot \text{m}^{-2} \cdot \text{d}^{-1}$ ) being approximately double with respect to T2 ( $12.6 \text{ g CO}_2 \cdot \text{m}^{-2} \cdot \text{d}^{-1}$ ) and T3 ( $10.7 \text{ g CO}_2 \cdot \text{m}^{-2} \cdot \text{d}^{-1}$ ) observed in July. The same trend for chemical oxygen demand (COD) removal efficiency, decreasing from T1 to T3, was observed. Notwithstanding this behavior, the final effluent quality was very satisfactory, with an average value of COD removal efficiency above 90%.

**Keywords:** wastewater treatment; carbon dioxide emission; clogging; horizontal flow; *Phragmites australis*



**Citation:** Sacco, A.; Sciuto, L.; Licciardello, F.; Cirelli, G.L.; Milani, M.; Barbera, A.C. Effects of Solids Accumulation on Greenhouse Gas Emissions, Substrate, Plant Growth and Performance of a Mediterranean Horizontal Flow Treatment Wetland. *Environments* **2023**, *10*, 30. <https://doi.org/10.3390/environments10020030>

Academic Editor: Jan Vymazal

Received: 5 December 2022

Revised: 30 January 2023

Accepted: 8 February 2023

Published: 13 February 2023



**Copyright:** © 2023 by the authors. Licensee MDPI, Basel, Switzerland. This article is an open access article distributed under the terms and conditions of the Creative Commons Attribution (CC BY) license (<https://creativecommons.org/licenses/by/4.0/>).

## 1. Introduction

Treatment wetlands (TWs) are systems increasingly used worldwide to treat different types of wastewater (WW) [1] by removing mineral and organic pollutants through both physical and biochemical processes [2–4]. Besides the reusable effluent, they integrate water service management and reduce the resource demands for freshwater [5]. However, managers often have to face pore clogging, a complex and challenging phenomenon that affects TWs during their operational life [6]. In addition, the new century's challenges, namely global warming and climate change, have pushed several authors to study TWs also in terms of environmental sustainability. It is well recognized that in such nature-based systems, organic matter is removed through carbon dioxide ( $\text{CO}_2$ ) and methane ( $\text{CH}_4$ ) evolution, and they can act as a carbon (C) sink or source. More than 200 papers have been published in international peer-reviewed journals [4,7] considering  $\text{CO}_2$  emission and sequestration, as well as  $\text{CH}_4$  emissions in TW concerning numerous factors: TW types; meteorological [8], hydrological [9], operational, and lifespan conditions [10]; and

vegetation [4]. In addition, some authors highlighted that the permeability variation of a TW substrate would affect greenhouse gas (GHG) flows and their interactions with the underlying groundwater [11,12]. Moreover, pore clogging generally causes the rise of the water table. This TW condition creates anaerobic (anoxic) soil, which can store  $\text{CO}_2$  and release  $\text{CH}_4$  by decreasing the decomposition rate [13]. In addition, aerobic degradation is the predominant process responsible for organic matter removal, and the accumulation of insoluble organic matter in TWs can reduce the organic matter removal rate [14], even if the total treatment capacity of a partially clogged horizontal flow (HF) unit could remain satisfactory [15]. To the best of our knowledge, no studies have been conducted on the effects of solids accumulation on GHG emissions in Mediterranean conditions. To fill this gap, the proposed study aims to evaluate the effects of solids accumulation on the GHG emissions, substrate, plant growth, and performance of a Mediterranean eight-year-old full-scale HF-TW planted with *Phragmites australis*.

## 2. Materials and Methods

### 2.1. Study Site and Experimental Design

This study was performed in a full-scale HF-TW (Figure 1) located in Catania (South Italy,  $37^\circ 26' \text{ N}$ ;  $15^\circ 01' \text{ E}$ ) in the Mediterranean basin. The hybrid TW consists of three in-series connected units, one HF, and two vertical flows (VF1 and VF2). The TW has been operating since 2014 as a support for the primary sequence batch reactor (SBR) system. VF1 and VF2 allow for the treatment WWs and nitrification of ammonia to nitrate. The HF unit, with a surface area of  $400 \text{ m}^2$  and a project flow rate of  $30 \text{ m}^3 \cdot \text{d}^{-1}$  (split into two batch phases every day), serves as the tertiary treatment step. It has been designed to reduce organic matter and suspended solids (SS) concentrations. The HF filtering unit is 1% slope, 0.6 m deep on average, filled with volcanic gravel (8–10 mm, 0.41 porosity) and planted with *P. australis* at a density of approximately 4 rhizomes per  $\text{m}^2$ . During the experiments, the water table was kept constant at 0.30 m from the HF surface to facilitate substrate sampling operations. To collect data, besides the inlet (P0) and the outlet (P10), nine observation points, three 8.5-m-long transects (T1 at 8.5 m, T2 at 17 m, and T3 at 25.5 m), were considered. Each transect was equipped with three piezometers of 0.30 m depth inserted inside the HF unit and placed at a 3 m distance from each other. Observed data were calculated by averaging the three observation points in each transect (from P1 to P9) at the same distance from the inlet, since no significant difference ( $p < 0.05$ ) was observed in the three sampling points for each distance for the studied parameters. The T1 area was afflicted by a severe hydraulic conductivity reduction ( $K_s = 660 \text{ m} \cdot \text{d}^{-1}$ ) in comparison to T2 and T3, which showed  $K_s = 6508 \text{ m} \cdot \text{d}^{-1}$  and  $K_s = 6104 \text{ m} \cdot \text{d}^{-1}$ , respectively [16]. The HF vegetation has been harvested every year (at the end of January) when the shoot vegetation is maximum.

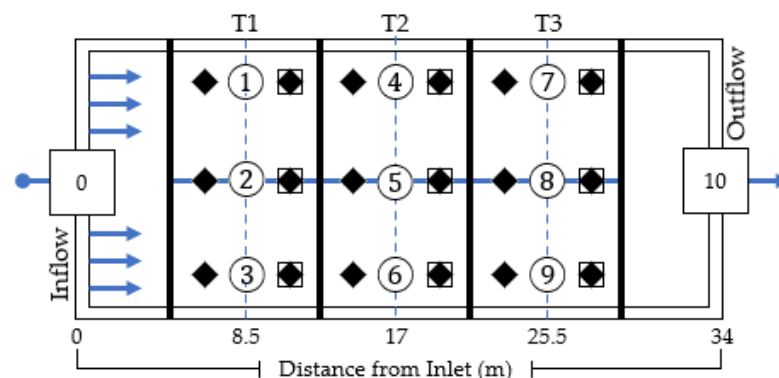


**Figure 1.** HF layout and experimental setup—black diamonds are bulk substrate sampling points; circles are piezometers, squares are aboveground biomass sampling points, and numbers are wastewater sampling points.

## 2.2. Weather Data

A weather station (Campbell Scientific—General Research-Grade Weather Station—GRWS100), able to record different climatic variables, was installed close to the TW plant to record the following meteorological data: air temperature, wind speed and direction, rainfall, and relative humidity. The HF influent flow rate and the HF effluent WW discharge volume, combined with precipitation data measured by the meteorological station, were used to estimate the evapotranspiration (ET) rates of *P. australis* during the vegetative period. The ET was calculated using a water balance approach [17].

## 2.3. Water Quality

The water flow rate was daily collected and recorded at the inlet and outlet using a flow-measurement device (B-Meters MUT 2200 EL). WW samples were collected at the inflow and outflow wells and at the nine piezometers installed in the HF unit. Biochemical oxygen demand (BOD<sub>5</sub>, mg·L<sup>-1</sup>), chemical oxygen demand (COD, mg L<sup>-1</sup>), total nitrogen (TN, mg L<sup>-1</sup>), total phosphorous (P, mg L<sup>-1</sup>), and total suspended solids (TSS, mg L<sup>-1</sup>) were calculated according to the reported method [18]. The removal efficiency (*RE*, %) of the system was calculated as follows (1):

$$RE(\%) = \left(1 - \frac{C_{out}}{C_{in}}\right) \cdot 100 \quad (1)$$

where  $C_{out}$  and  $C_{in}$  are the pollutant concentrations in the effluent and inflow points, respectively. In particular, the COD, *RE*, was evaluated also for each transect.

## 2.4. Accumulated Material Characterization and Vegetation Study

Substrate samples mixed with belowground biomass and organic matter were collected at 2 points around each piezometer ( $n = 18$  samples). A depth of 0.30 m was explored as most of the plant root apparatus was concentrated in the system's upper layer [19]. At each sampling point, a 0.20-m-diameter by 0.30-m-long sharp-end steel tube was inserted in the unit substrate to avoid the collapse of the lateral wall inside the hole and to collect the material samples. The steel tube was inserted in the unsaturated zone of the HF system surface. Then, the bulk sample inside the tube was extracted by a soil scoop (0.005 m<sup>3</sup>). Laboratory analyses were performed to characterize the sampled material in terms of concentrations of accumulated total solids (TS, g·m<sup>-3</sup>), volatile solids (VS, g·m<sup>-3</sup>), and plant root biomass (PRB, g·m<sup>-3</sup>) [20]. Moreover, in each transect, three 1 m<sup>2</sup> parcels were outlined to study *P. australis* aboveground volume in terms of the number, height, and circumference of culms from January to December 2021.

## 2.5. Greenhouse Gas Emissions

The monitoring activities were performed from January to December 2021. Daily CO<sub>2</sub> emissions were measured after plant cutting when shoot vegetation coverage was = 0% up to the end of the year. The static stationary chamber technique [3,21] was used to estimate in situ CO<sub>2</sub> emissions in T1, T2, and T3 of the HF unit. Further details of the constructive and operational features, apparatus setting, and calibration are described by Barbera et al. [3] and Zhao et al. [21]. The chamber was positioned with its bottom part (0.2 m) permanently inserted in each fixed HF sampling point to calculate cumulative CO<sub>2</sub> daily emissions. For each transect, two replicated measures around each piezometer were acquired. Theoretical CH<sub>4</sub> emissions were calculated as a function of the BOD<sub>5</sub> loaded into the HF unit and its related emission, as suggested by Barbera et al. [22]. This method is defined as a good practice approach for countries with limited data [23]. The EF was obtained using the following Equation (2).

$$EF = B_0 \cdot MCF \quad (2)$$

where  $B_0$  indicates the maximum  $\text{CH}_4$  generation capacity. In this study, a default value of  $0.6 (\text{kg}\cdot\text{CH}_4)\cdot(\text{kg}\cdot\text{BOD}_5)^{-1}$  has been applied [24]. MCF indicates the  $\text{CH}_4$  correction factor for TW type ( $MCF = 0.1$  for HF-TW [24]).

## 2.6. Data Analysis

Statistical analysis in this study was performed using *Minitab* software v.21.1.  $\text{CO}_2$  emissions and organic biomass fraction among T1, T2, and T3 were evaluated by analysis of variance (ANOVA). The non-parametric Kruskal–Wallis test with  $p < 0.05$  was performed to check the  $\text{CO}_2$  emission differences and the aboveground biomass growing in the three transects. Statistical significance between two average values of TS, VS, PRB was tested by a two-tailed  $t$  test ( $p = 0.05$ ), assuming a normal distribution for these variables. The multiple linear regression model was applied to check the relationship between the observed  $\text{CO}_2$  emissions and the weather variables. According to the influent and effluent concentrations of  $\text{BOD}_5$ , COD,  $\text{NH}_4^+\text{-N}$ , TN, TP, and TSS, the statistical difference in the average RE values was calculated using the ANOVA.

## 3. Results and Discussion

### 3.1. Weather Data

The meteorological data recorded during the experimental period showed typical characteristics of Mediterranean environments, with average annual rainfall of approximately 626 mm and an average annual air temperature of  $18.3\text{ }^\circ\text{C}$ , ranging from a minimum of  $9.8\text{ }^\circ\text{C}$  up to a maximum of  $31.6\text{ }^\circ\text{C}$ , with average relative humidity of 39.8%. The discussed timespan was characterized by cumulative solar radiation of  $214.34\text{ MJ}\cdot\text{m}^{-2}\cdot\text{d}^{-1}$  and an average wind speed of around  $1.72\text{ m}\cdot\text{s}^{-1}$ , with a prevailing wind direction of  $247.50^\circ$  north. The average daily ET was  $6.80\text{ mm}\cdot\text{d}^{-1}$  and showed the highest value ( $14.61\text{ mm}\cdot\text{d}^{-1}$ ) at the end of July. The lowest value was recorded at the end of January ( $0.96\text{ mm}\cdot\text{d}^{-1}$ ). As highlighted in several studies [4,8,25,26], the environmental conditions may influence directly and indirectly the vegetation development, the microbial communities, and their level of activity. The linear regression analysis performed in this study suggests a linear association of observed  $\text{CO}_2$  emissions with both the average air temperature ( $R^2 = 0.75$ ) and the average solar radiation ( $R^2 = 0.63$ ) recorded during the observation period (Figure 2). This result agrees with the positive correlation highlighted in more than 200 reviewed papers [4]. Instead, no significative regression was found between the  $\text{CO}_2$  emissions and rainfall or humidity variables.

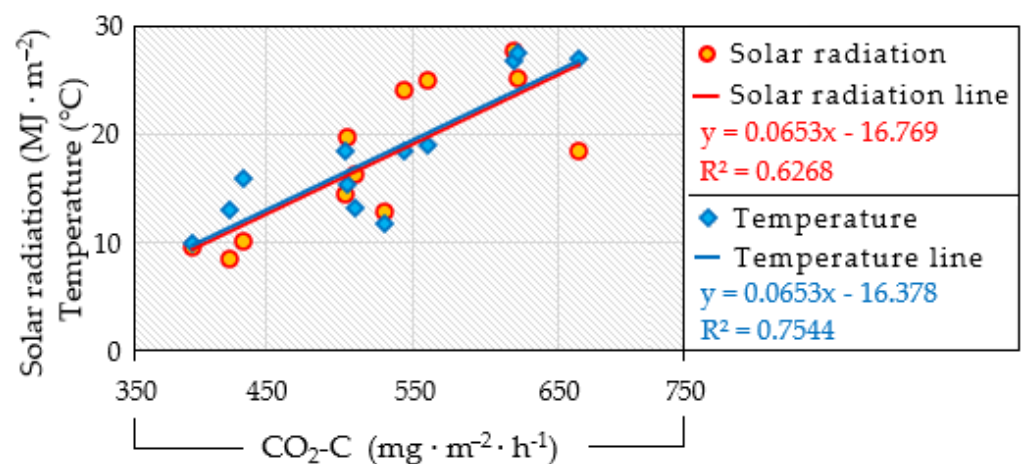


**Figure 2.** Linear regressions between the average monthly  $\text{CO}_2$  emissions from the HF unit and the average air temperature values (blue line) and the average solar radiation values (red line) documented during the observation period (January–December 2021). Yellow circles and blue diamonds are solar radiation and temperature data, respectively.

It was found that there was a significant correlation between the average air temperature and CO<sub>2</sub> emissions in a pilot-plant scale HF-TW vegetated with *Chrisopogon zizanioides* and *P. australis* [3,4]. Moreover, Zhu et al. [27] reported a positive correlation of CO<sub>2</sub> flow rates through the culms with solar radiation in a HF-TW unit vegetated with *P. australis*. Regarding CO<sub>2</sub>, similarly, it was highlighted that there was a positive correlation with solar radiation but only for *Cyperus papyrus* [3,4], supporting the suggestion that not only the vegetation's presence has a significant impact on the GHG emissions from TW, but also the plant genotype [28,29].

### 3.2. Water Quality

COD removal increased significantly from T1 to T2 to T3 for the whole observation period. In T1, the range of COD removal monthly variability was 6–14%, with a mean value of 10%; in T2, it was 14–40%, with a mean value of 24%; in T3, it was 17–58%, with a mean value of 33% (Figure 3). The lowest COD-RE observed in the T1 transect could be due to the pore clogging phenomenon, which causes a unit useful volume loss and a rise in the water table, generating anaerobic (anoxic) zones. As is well known, aerobic degradation is the predominant process responsible for COD removal, and the accumulation of insoluble organic matter in the HF unit may reduce the COD removal rate [14]. This behavior is in line with a study that found that the amount of COD degradation is related to the effective porous volume of the filler [30]. Notwithstanding the lower COD-RE in the first part of the HF unit, the effluent quality was good during the whole observation period, with an average value of COD-RE above 90% [31,32]. In fact, the treatment performance of a partially clogged HF unit may remain satisfactory [15]. Table 1 shows the average concentrations and the RE of the main pollutants obtained from the water sample analysis collected at the inflow and outflow of the HF unit during the monitoring campaign (2021).

**Table 1.** Average concentrations and removal efficiencies with standard deviation ( $\pm$ SD) of the physicochemical parameters detected at the inflow (in) and outflow (out) of the HF-TW during the experimental period (January–December 2021).

Water Quality Parameter	HF In (mg·L <sup>-1</sup> ) ( $\pm$ SD, n = 12)	HF Out (mg·L <sup>-1</sup> ) ( $\pm$ SD, n = 12)	Removal Efficiency (%) ( $\pm$ SD, n = 12)
COD	164.4 ( $\pm$ 17.1)	38.4 ( $\pm$ 13.1)	76.6 ( $\pm$ 7.3)
BOD <sub>5</sub>	129.11 ( $\pm$ 28.5)	8.2 ( $\pm$ 4.3)	93.6 ( $\pm$ 1.8)
TSS	62.2 ( $\pm$ 39.4)	4 ( $\pm$ 5.8)	99 ( $\pm$ 0.8)
N-NH <sub>4</sub>	12.8 ( $\pm$ 10.6)	0.1 ( $\pm$ 0.1)	99 ( $\pm$ 0.4)
Total N	76 ( $\pm$ 28.5)	26.9 (25.8)	74.3 ( $\pm$ 30)
Total P	16.6 ( $\pm$ 9.1)	10.2 ( $\pm$ 11.1)	54 ( $\pm$ 15)

Pollutant concentrations of the final effluent were low ( $4 \pm 5.8$  mg·L<sup>-1</sup> of TSS,  $0.1 \pm 0.1$  mg·L<sup>-1</sup> of N-NH<sub>4</sub><sup>+</sup>,  $26.9 \pm 25.8$  mg·L<sup>-1</sup> of N<sub>tot</sub>, and  $10.2 \pm 11.1$  mg·L<sup>-1</sup> of P<sub>tot</sub>), notwithstanding the high initial concentrations at the inlet stage ( $62.2 \pm 39.4$  mg·L<sup>-1</sup> of TSS;  $12.8 \pm 10.6$  mg·L<sup>-1</sup> of N-NH<sub>4</sub><sup>+</sup>,  $76 \pm 28.5$  mg·L<sup>-1</sup> of N<sub>tot</sub>, and  $16.6 \pm 9.1$  mg·L<sup>-1</sup> of P<sub>tot</sub>). Therefore, results evidenced the key role of the HF unit, which provided an efficient reduction in TSS (up to  $99 \pm 0.8\%$ ), N-NH<sub>4</sub><sup>+</sup> (up to  $99 \pm 0.4\%$ ), N<sub>tot</sub> (up to  $74.3 \pm 30\%$ ), and P<sub>tot</sub> (up to  $54 \pm 15\%$ ). The effluent quality was outstanding, and the BOD<sub>5</sub>, COD, and TSS values were below the Italian law discharge limits ( $35$  and  $125$  mg·L<sup>-1</sup>, respectively). The HF unit provided a very high average reduction in TSS and BOD<sub>5</sub>, allowing for the limits fixed by the Italian law to be respected. The high TN reduction confirmed that both processes (nitrification and denitrification) were efficient.

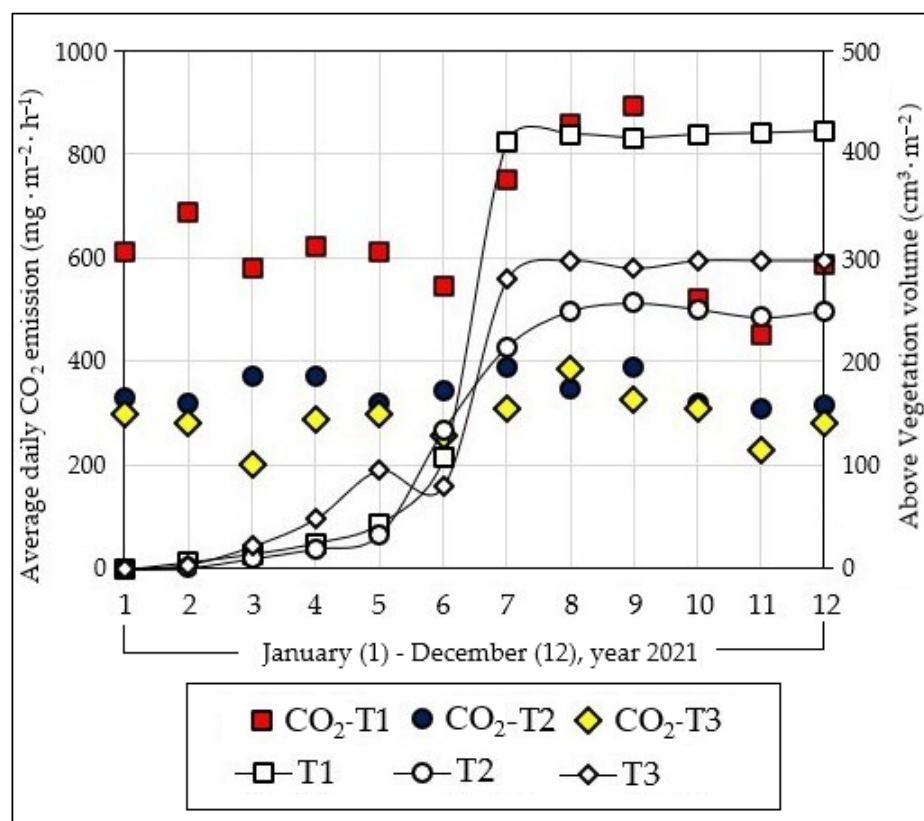


**Figure 3.** Temporal trend and comparison between the aboveground vegetation volume ( $\text{cm}^3$  per  $\text{m}^2$ ) and  $\text{CO}_2$  emissions ( $\text{mg}\cdot\text{m}^{-2}\cdot\text{h}^{-1}$ ) documented in the three transects during the experimental campaign. Red squares, blue circles, and yellow diamonds are the average values of  $\text{CO}_2$  emissions observed in T1, T2, and T3, respectively, during 2021. White squares, circles, and diamonds are average values of the aboveground vegetation volume of *Phragmites australis* documented in 2021.

### 3.3. Accumulated Material Characterization

In T1, TS concentrations varied between  $3088.61$  and  $5646.41 \text{ g}\cdot\text{m}^{-3}$  with an average value of  $4320.48 \pm 471.45 \text{ g}\cdot\text{m}^{-3}$  ( $\text{CV} = 0.10$ ). The VS concentration varied from  $1550.07$  to  $2157.12 \text{ g}\cdot\text{m}^{-3}$  with an average value of  $1355 \pm 115.15 \text{ g}\cdot\text{m}^{-3}$  ( $\text{CV} = 0.08$ ), and the volatile fraction accounted for 51% of the total TS concentration. T2 showed a TS concentration ranging between  $656.01$  and  $1152.43 \text{ g}\cdot\text{m}^{-3}$  with an average value of  $920.48 \pm 77.28 \text{ g}\cdot\text{m}^{-3}$  ( $\text{CV} = 0.08$ ); meanwhile, T3 is characterized by a TS concentration that ranges between  $467.89$  and  $1055.08 \text{ g}\cdot\text{m}^{-3}$  with an average value of  $846.48 \pm 61.4 \text{ g}\cdot\text{m}^{-3}$  ( $\text{CV} = 0.12$ ). The volatile fraction in T2 and T3 accounted for 27.7% and 25% of the total TS concentration, respectively. The higher VS average concentration value in T1 with respect to the rest of the HF unit may be explained as an effect of the organic matter accumulation close to the inlet area. Moreover, the VS average value's trend with respect to the distance from the inlet has a strong negative correlation ( $R^2 = -0.98$ ) with the  $K_s$  one (Figure 4). Similarly, other authors [19] observed a significant increase in VS close to this zone. This result is in line with the  $K_s$  reduction observed close the inlet zone [16], which has been highlighted as an expected consequence of organic matter accumulation due to the WW type and supply also in other studies [32,33]. TS and VS did not have significant temporal trends during the observation period.

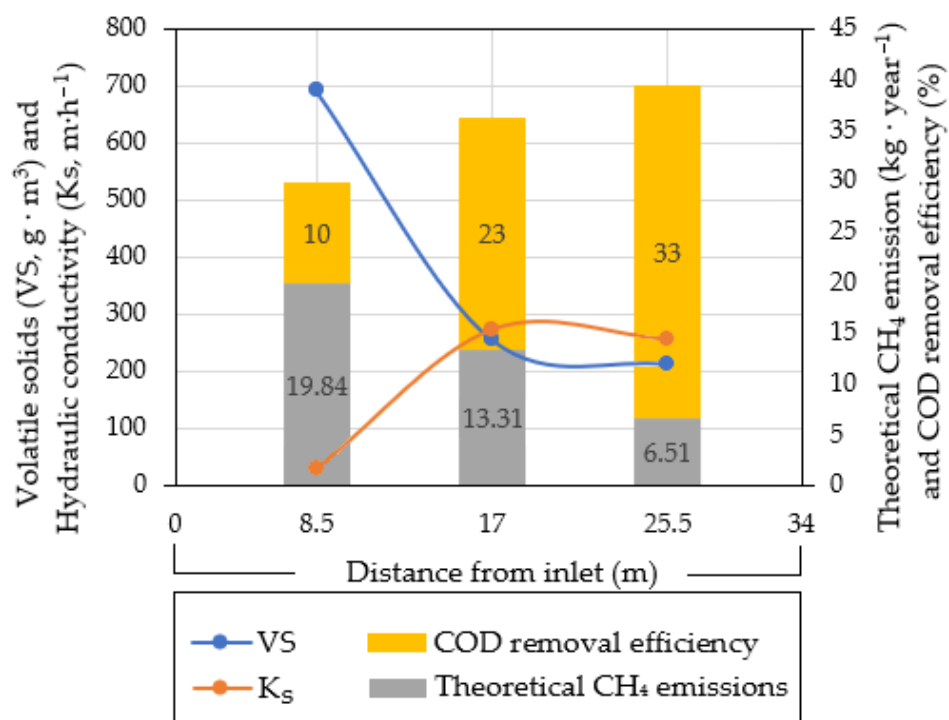


**Figure 4.** Data comparison with the distance from the inlet of volatile solid average values (VS, g·m<sup>-3</sup>); K<sub>s</sub> average values (m·h<sup>-1</sup>) reported [16] (m·h<sup>-1</sup>), COD removal efficiency (%), and theoretical CH<sub>4</sub> emission (kg·year<sup>-1</sup>).

### 3.4. *Phragmites australis* Growth

The monthly aboveground vegetation volume (calculated from the number of culms, height, and circumference) showed an expected increasing trend from February to July. This trend was almost similar in the three transects from February to May (Figure 3). However, a higher growth rate was observed in T1 starting from June, and it rose until August (Figure 3). The lowest values of the monthly above vegetation volume were observed in the T1 area, which was affected by pore clogging. The PRB measured at 0.3 m belowground depth followed the same trend, with values decreasing from T1 (5646.8 g m<sup>-3</sup>) to T2 (1650.2 g m<sup>-3</sup>) and finally to T3 (656.0 g m<sup>-3</sup>); no significant temporal variation was observed during the experimental campaign.

### 3.5. Greenhouse Gas Emissions

CO<sub>2</sub> emissions increased during the summer, when the temperature and solar radiation were higher than in the rest of the year (Figure 2). CO<sub>2</sub> emissions were significantly different among T1, T2, and T3, with maximum monthly values in T1 (21.4 g·CO<sub>2</sub>·m<sup>-2</sup>·d<sup>-1</sup>) being approximately double with respect to T2 (11.3 g·CO<sub>2</sub>·m<sup>-2</sup>·d<sup>-1</sup>) and T3 (10.7 g·CO<sub>2</sub>·m<sup>-2</sup>·d<sup>-1</sup>) observed in July (Figure 3). Minimum monthly values (10.8 g·CO<sub>2</sub>·m<sup>-2</sup>·d<sup>-1</sup>) in T1, 7.4 g·CO<sub>2</sub>·m<sup>-2</sup>·d<sup>-1</sup> in T2, and 4.8 g·CO<sub>2</sub>·m<sup>-2</sup>·d<sup>-1</sup> in T3) were observed mainly in November. T2 and T3 had a similar trend, with lower differences observed between summer and winter months compared to those observed for T1 (Figure 3). The seasonal trend observed for CO<sub>2</sub> in T1 agrees with that reported by several authors [7,34–37]. In semi-arid Mediterranean conditions, there is an average CO<sub>2</sub> daily emission value varying between 0.8 ± 0.1 g·CO<sub>2</sub>·m<sup>-2</sup>·d<sup>-1</sup> during the winter season and 24.9 ± 0.6 g·CO<sub>2</sub>·m<sup>-2</sup>·d<sup>-1</sup> in the summer season [3]. A similar seasonal tendency of CO<sub>2</sub> emissions (varying from 11.1 to 49.0 g·CO<sub>2</sub>·m<sup>-2</sup>·d<sup>-1</sup>) has been observed in another Mediterranean HF-TW vegetated with *P. australis* under anaerobic conditions [38]. Moreover, Picek and co-authors [28] reported CO<sub>2</sub> emissions varying between 0.4 and 27.2 g·CO<sub>2</sub>·m<sup>-2</sup>·d<sup>-1</sup> during summer and fall in an HF-TW with *P. australis* that treated combined sewage and stormwater runoff, but no

significant differences were highlighted by these authors when comparing the inlet and the outlet zones. In this study, the seasonal trend observed for CO<sub>2</sub> and the *P. Australis* volume was similar, with an R<sup>2</sup> equal to 0.74 for T1, 0.65 for T2, and 0.74 for T3. This could indicate that vegetation growth is responsible for the CO<sub>2</sub> emissions increase recorded during the summer season. The crucial role of vegetation growth in CO<sub>2</sub> emissions has been reported by numerous authors [4,39]. For example, Picek et al. [28] observed that CO<sub>2</sub> emissions gradually declined toward the end of the growing season. Additionally, they demonstrated that plants are an essential source of available carbon for the microorganisms in TWs. This carbon is further transformed into gaseous forms and increases carbon emissions from TWs. In this study, it has been highlighted that CH<sub>4</sub> emissions followed the trend of VS (Figure 4), with values decreasing from T1 (equal to 19.8 kg·CH<sub>4</sub>·year<sup>-1</sup>) to T2 (3.3 kg·CH<sub>4</sub>·year<sup>-1</sup>) and T3 (6.5 kg·CH<sub>4</sub>·year<sup>-1</sup>). The highest theoretical CH<sub>4</sub> emissions in T1 are probably due to anaerobic bacteria (methanogens) that increase in the HF unit's waterlogged anoxic part. Similarly, Liikanen et al. [8] measured higher methane emissions in the HF inlet zone (10 mg·CH<sub>4</sub>·m<sup>-2</sup>·d<sup>-1</sup>) than in the HF outlet zone (4.4 mg·CH<sub>4</sub>·m<sup>-2</sup>·d<sup>-1</sup>). This result may be explained by the HF influent loading [40], also resulting in the greater availability of organic substrates for bacterial biomass growth associated with the inlet zone.

#### 4. Conclusions

Both contributors to C emissions (CO<sub>2</sub>-C and CH<sub>4</sub>-C) were the highest in the inlet zone (T1). This behavior may be explained by the different processes acting simultaneously in the TW. Firstly, the highest values of CO<sub>2</sub> emissions can be explained by the *P. Australis* growth rate, which was higher in T1 than in the rest of the HF system during summer, when the temperature and solar radiation increased. In particular, the increasing monthly aboveground vegetation volume trend was almost similar in the three transects from February to May; an increasing rate, higher in T1, was instead observed starting from June, and it rose in July. Similar to the monthly aboveground vegetation volume, belowground biomass measured at 0.3 m depth also decreased from T1 to T2 and T3. Secondly, pore clogging explained the highest CH<sub>4</sub> emissions in T1, due to the presence of anaerobic bacteria (methanogens) that proliferated in this waterlogged, anoxic part of the TW. In fact, also the solids volatile fraction was higher in T1 (around 3.5 and 4 times) than in T2 and T3. Moreover, the pore clogging caused a K<sub>s</sub> reduction in T1 (around one order of magnitude) compared to T2 and T3, and an observed COD removal increase from T1 to T2 to T3 for the whole observation period. Notwithstanding the negative effects of the pore clogging observed in the first part of the HF unit, the effluent quality was very satisfactory over the entire observation period, with the average value of COD removal efficiency above 90%. Further investigations will be carried out with the aim of assessing the potential effects of pore clogging on the TW carbon balance.

**Author Contributions:** The authors contributed with equal efforts to the realization of the paper. They were individually involved as follows: writing—review, editing, data curation, and investigation: A.S., F.L. and L.S.; conceptualization, methodology, and formal analysis: A.S., A.C.B. and G.L.C.; software, validation, and resources: M.M. and L.S.; supervision: G.L.C. and A.C.B. All authors have read and agreed to the published version of the manuscript.

**Funding:** This work has been funded by (1) the University of Catania PIA no di inCentivi per la Ricerca di Ateneo 2020/2022—Linea di Intervento 3 “Starting Grant” (15084506-75004/1); (2) the International Doctorate in Agricultural, Food, and Environmental Science—Di3A—University of Catania; (3) PON “RICERCA E INNOVAZIONE” 2014–2020, Azione II—Obiettivo Specifico 1b—Progetto “Miglioramento delle produzioni agroalimentari mediterranee in condizioni di carenza di risorse idriche”—WATER4AGRI FOOD. Project number: ARS01\_00825. CUP B64I20000160005.

**Data Availability Statement:** Data available on request from the authors.

**Acknowledgments:** We thank IKEA® Retail Italia of Catania and its technical personnel for their comprehensive availability and assistance during the monitoring activities.

**Conflicts of Interest:** The authors declare no conflict of interest. The funders had no role in the design of the study; in the collection, analyses, or interpretation of data; in the writing of the manuscript, or in the decision to publish the results.

## References

1. Vymazal, J. The use constructed wetlands with horizontal sub-surface flow for various types of wastewaters. *Ecol. Eng.* **2009**, *35*, 1–17. [[CrossRef](#)]
2. Vymazal, J. The use of hybrid constructed wetlands for wastewater treatment with special attention to nitrogen removal: A review of a recent development. *Water Res.* **2013**, *47*, 4795–4811. [[CrossRef](#)] [[PubMed](#)]
3. Barbera, A.C.; Borin, M.; Ioppolo, A.; Cirelli, G.L.; Maucieri, C. Carbon dioxide emissions from horizontal sub-surface constructed wetlands in the Mediterranean Basin. *Ecol. Eng.* **2014**, *64*, 57–61. [[CrossRef](#)]
4. Maucieri, C.; Barbera, A.C.; Vymazal, J.; Borin, M. A review on the main affecting factors of greenhouse gases emission in constructed wetlands. *Agr. For. Meteorol.* **2017**, *236*, 175–193. [[CrossRef](#)]
5. Ventura, D.; Ferrante, M.; Copat, C.; Grasso, A.; Milani, M.; Sacco, A.; Licciardello, F.; Cirelli, G.L. Metal removal processes in a pilot hybrid constructed wetland for the treatment of semi-synthetic stormwater. *Sci. Total Environ.* **2021**, *754*, 142221. [[CrossRef](#)]
6. Sacco, A.; Cirelli, G.L.; Ventura, D.; Barbagallo, S.; Licciardello, F. Hydraulic performance of horizontal constructed wetlands for stormwater treatment: A pilot-scale study in the Mediterranean. *Ecol. Eng.* **2022**, *169*, 106290. [[CrossRef](#)]
7. Mander Ülo Dotro, G.; Ebie, Y.; Towprayoon, S.; Chiemchaisri, C.; Nogueira, S.F.; Jamsranjav, B.; Kasak, K.; Truu, J.; Tournebize, J.; Mitsch, W.J. Greenhouse gas emission in constructed wetlands for wastewater treatment: A review. *Ecol. Eng.* **2014**, *66*, 19–35. [[CrossRef](#)]
8. Liikanen, A.; Huttunen, J.T.; Karjalainen, S.M.; Heikkinen, K.; Väisänen, T.S.; Nykänen, H.; Martikainen, P.J. Temporal and seasonal changes in greenhouse gas emissions from a constructed wetland purifying peat mining runoff waters. *Ecol. Eng.* **2006**, *26*, 241–251. [[CrossRef](#)]
9. Altor, A.E.; Mitsch, W.J. Pulsing hydrology, methane emissions and carbon dioxide fluxes in created marshes: A 2-year ecosystem study. *Wetlands* **2008**, *28*, 423–438. [[CrossRef](#)]
10. Zemanová, K.; Pícek, T.; Dušek, J.; Edwards, K.; Šantrůčková, H. Carbon, nitrogen and phosphorus transformations are related to age of a constructed wetland. *Water Air Soil Pollut.* **2010**, *207*, 39–48. [[CrossRef](#)]
11. Dzakpasu, M.; Scholz, M.; Harrington, R.; Jordan, S.N.; McCarthy, V. Characterising infiltration and contaminant migration beneath earthen-lined integrated constructed wetlands. *Ecol. Eng.* **2012**, *41*, 41–51. [[CrossRef](#)]
12. Dzakpasu, M.; Scholz, M.; Harrington, R.; McCarthy, V.; Jordan, S. Groundwater quality impacts from a full-scale integrated constructed wetland. *Groundw. Monit. Remediat.* **2014**, *34*, 51–64. [[CrossRef](#)]
13. Rosli, F.A.; Lee, K.E.; Goh, C.T.; Mokhtar, M.; Latif, M.T.; Goh, T.L.; Simon, N. The use of constructed wetlands in sequestering carbon: An overview. *Nat. Environ. Pol. Tech.* **2017**, *16*, 813–819.
14. Vymazal, J. Removal of BOD<sub>5</sub> in constructed wetlands with horizontal sub-surface flow: Czech experience. *Water Sci. Technol.* **1999**, *40*, 133–138. [[CrossRef](#)]
15. Vymazal, J. Does clogging affect long-term removal of organics and suspended solids in gravel-based horizontal subsurface flow constructed wetlands? *Chem. Eng. J.* **2018**, *331*, 663–674. [[CrossRef](#)]
16. Licciardello, F.; Sacco, A.; Barbagallo, S.; Ventura, D.; Cirelli, G.L. Evaluation of different methods to assess the hydraulic behavior in horizontal treatment wetlands. *Water* **2020**, *12*, 2286. [[CrossRef](#)]
17. Milani, M.; Marzo, A.; Toscano, A.; Consoli, S.; Cirelli, G.L.; Ventura, D.; Barbagallo, S. Evapotranspiration from horizontal subsurface flow constructed wetlands planted with different perennial plant species. *Water* **2019**, *11*, 2159. [[CrossRef](#)]
18. Baird, R.B.; Eaton, A.D.; Rice, E.W. *Standard Methods for the Examination of Water and Wastewater*, 23rd ed.; American Public Health Association, American Water Works Association, Water Environment Federation: Washington, DC, USA, 2017.
19. Aiello, R.; Bagarello, V.; Barbagallo, S.; Iovino, M.; Marzo, A.; Toscano, A. Evaluation of clogging in full-scale subsurface flow constructed wetlands. *Ecol. Eng.* **2018**, *95*, 505–513. [[CrossRef](#)]
20. APHA-AWWA-WEF. *Standard Methods for Examination of Water and Wastewater*, 22nd ed.; American Public Health Association: Washington, DC, USA, 2012.
21. Zhao, P.; Hammerle, A.; Zeeman, M.; Wohlfahrt, G. On the calculation of daytime CO<sub>2</sub> fluxes measured by automated closed transparent chambers. *Agr. For. Meteorol.* **2018**, *263*, 267–275. [[CrossRef](#)] [[PubMed](#)]
22. Barbera, A.C.; Borin, M.; Cirelli, G.L.; Toscano, A.; Maucieri, C. Comparison of carbon balance in Mediterranean pilot constructed wetlands vegetated with different C<sub>4</sub> plant species. *Environ. Sci. Pollut. Res.* **2015**, *22*, 2372–2383. [[CrossRef](#)] [[PubMed](#)]
23. IPCC. Guidelines for national greenhouse gas inventories. In *The National Greenhouse Gas Inventories Programme*; Eggleston, H.S., Buendia, L., Miwa, K., Ngara, T., Tanabe, K., Eds.; The Intergovernmental Panel on Climate Change: Hayama, Japan, 2006.
24. Paredes, M.G.; Güereca, L.P.; Molina, L.T.; Noyola, A. Methane emissions from stabilization ponds for municipal wastewater treatment in Mexico. *J. Int. Environ. Sci.* **2015**, *12*, 139–153. [[CrossRef](#)]
25. IPCC 2013. *Supplement to the 2006 IPCC Guidelines for National Greenhouse Gas Inventories: Wetlands*; Hiraishi, T., Krug, T., Tanabe, K., Srivastava, N., Baasansuren, J., Fukuda, M., Troxler, T.G., Eds.; IPCC: Geneva, Switzerland, 2013.
26. Wang, Y.; Yang, H.; Ye, C.; Chen, X.; Xie, B.; Huang, C.; Zhang, J.; Xu, M. Effects of plant species on soil microbial processes and CH<sub>4</sub> emission from constructed wetlands. *Environ. Pol.* **2013**, *174*, 273–278. [[CrossRef](#)]

27. Zhu, N.; An, P.; Krishnakumar, B.; Zhao, L.; Sun, L.; Mizuochi, M.; Inamori, Y. Effect of plant harvest on methane emission from two constructed wetlands designed for the treatment of wastewater. *J. Environ. Manag.* **2007**, *85*, 936–943. [[CrossRef](#)]
28. Pícek, T.; Čížková, H.; Dušek, J. Greenhouse gas emissions from a constructed wetland—Plants as important sources of carbon. *Ecol. Eng.* **2007**, *31*, 98–106. [[CrossRef](#)]
29. Ström, L.; Lamppa, A.; Christensen, T.R. Greenhouse gas emissions from a constructed wetland in southern Sweden. *Wet. Ecol. Manag.* **2007**, *15*, 43–50. [[CrossRef](#)]
30. Verville, J.H.; Hobbie, S.E.; Chapin, F.S.; Hooper, D.U. Response of tundra CH<sub>4</sub> and CO<sub>2</sub> flux to manipulation of temperature and vegetation. *Biogeochemistry* **1998**, *41*, 215–235. [[CrossRef](#)]
31. Xu, Q.; Chen, S.; Huang, Z.; Cui, L.; Wang, X. Evaluation of organic matter removal efficiency and microbial enzyme activity in vertical-flow constructed wetland systems. *Environments* **2016**, *3*, 26. [[CrossRef](#)]
32. Marzo, A.; Ventura, D.; Cirelli, G.L.; Aiello, R.; Vanella, D.; Rapisarda, R.; Barbagallo, S.; Consoli, S. Hydraulic reliability of a horizontal wetland for wastewater treatment in Sicily. *Sci. Total Environ.* **2018**, *636*, 94–106. [[CrossRef](#)] [[PubMed](#)]
33. Pedescoll, A.; Uggetti, E.; Llorens, E.; Granés, F.; García, D.; García, J. Practical method based on saturated hydraulic conductivity used to assess clogging in subsurface flow constructed wetlands. *Ecol. Eng.* **2009**, *35*, 1216–1224. [[CrossRef](#)]
34. Tanner, C.C.; Adams, D.D.; Downes, M.T. Methane Emissions from Constructed Wetlands Treating Agricultural Wastewaters. *J. Environ. Qual.* **1997**, *26*, 1056–1062. [[CrossRef](#)]
35. Johansson, A.E.; Gustavsson, A.M.; Öquist, M.G.; Svensson, B.H. Methane emissions from a constructed wetland treating wastewater—Seasonal and spatial distribution and dependence on edaphic factors. *Water Res.* **2004**, *38*, 3960–3970. [[CrossRef](#)]
36. Søvik, A.K.; Augustin, J.; Heikkinen, K.; Huttunen, J.T.; Necki, J.M.; Karjalainen, S.M.; Kløve, B.; Liikanen, A.; Mander, Ü.; Puustinen, M.; et al. Emission of the Greenhouse Gases Nitrous Oxide and Methane from Constructed Wetlands in Europe. *J. Environ. Qual.* **2007**, *35*, 2360–2373. [[CrossRef](#)]
37. Maltais-Landry, G.; Maranger, R.; Brisson, J.; Chazarenc, F. Greenhouse gas production and efficiency of planted and artificially aerated constructed wetlands. *Environ. Pollut.* **2009**, *157*, 748–754. [[CrossRef](#)]
38. Garcia, J.; Capel, V.; Castro, A.; Ruiz, I.; Soto, M. Anaerobic biodegradation tests and gas emissions from subsurface flow constructed wetlands. *Bioresour. Technol.* **2007**, *98*, 3044–3052. [[CrossRef](#)]
39. Maucieri, C.; Borin, M.; Milani, M.; Cirelli, G.L.; Barbera, A.C. Plant species effect on CO<sub>2</sub> and CH<sub>4</sub> emissions from pilot constructed wetlands in Mediterranean area. *Ecol. Eng.* **2019**, *134*, 112–117. [[CrossRef](#)]
40. Caselles-Osorio, A.; Puigagut, J.; Segú, E.; Vaello, N.; Granés, F.; García, D.; García, J. Solids accumulation in six full-scale subsurface flow constructed wetlands. *Water Res.* **2007**, *41*, 1388–1398. [[CrossRef](#)]

**Disclaimer/Publisher’s Note:** The statements, opinions and data contained in all publications are solely those of the individual author(s) and contributor(s) and not of MDPI and/or the editor(s). MDPI and/or the editor(s) disclaim responsibility for any injury to people or property resulting from any ideas, methods, instructions or products referred to in the content.